Theoretical Study of Microscopic Solvation of Lithium in Water Clusters: Neutral and Cationic $Li(H_2O)_n$ (n = 1−6 and 8)

Kenro Hashimoto* and Tetsuya Kamimoto

Contribution from the Computer Center, Tokyo Metropolitan University, 1-1 Minami-Ohsawa, Hachioji-shi, Tokyo 192-0397, Japan

Received August 6, 1997. Revised Manuscript Received December 8, 1997

Abstract: The structure, stability, and electronic state of $Li(H_2O)_n$ (n = 1−6 and 8) clusters have been investigated by an *ab initio* molecular orbital method, including electron correlation, and compared with those of their cations. The *interior* structure where the Li atom is surrounded by four H_2O molecules in the first shell and more in the second shell is found to be the most stable for both neutral and cationic $n \geq 4$ clusters. The size dependence of the vertical ionization potentials of $Li(H_2O)_n$ is in good agreement with the recent experiment. It decreases successively until $n = 4$ and becomes nearly constant for $n \geq 4$ being close to the bulk limit of vertical detachment energies of $(H_2O)_n^-$. The excess electron is separated from Li and distributed outside the first-shell cavity in $n \geq 4$ clusters. The electronic state of the clusters changes from a one-center atomic state for $n \leq 3$ to a two-center ionic state for $n \geq 4$ with a gradual localization of the excess electron. Dangling hydrogens interacting with the excess electron play a role as actuators of the *surface* state.

I. Introduction

Solvated electrons have attracted widespread attention for a long time. They have been studied extensively in physical, chemical, and biological fields.[1−3] An alkali metal atom in polar solvent clusters provides a good model for obtaining the microscopic aspect for this celebrated subject. It dissociates into a solvated positive ion and a separate solvated electron with a stepwise solvation. The electronic structure of the clusters is expected to change from a one-center atomic state to a two-center ionic state with an increasing number of solvent molecules. To understand the molecular mechanism of the alkali-metal dissolution producing the solvated electron in clusters, gas-phase studies such as the photoionization threshold measurement[4−6] and the negative ion photoelectron spectroscopy[6−10] of the size-selected solvated alkali atom clusters have been reported very actively.

Several years ago, Hertel's and Fuke's groups found that the ionization potentials (IPs) of $M(H_2O)_n$ (M = Na[4] and Cs[5]) clusters converged to the photoelectric threshold of ice[11] at n = 4 with no size dependence for larger n. The same peculiar size dependence in IPs has also been observed for hydrated Li clusters very recently.[6] This unusual behavior of the IPs for the hydrated alkali atom clusters has motivated theoretical challenges to elucidate the nature of these clusters.

Barnett and Landman[12] showed that the addition of water molecules to a Na atom resulted in a successive decrease in the IPs with a marked reduced variation for $n > 4$ by the local spin density (LSD) functional calculation. In their model, the Na valence electron in $n > 4$ clusters was expelled from the hydration cavity forming the delocalized surface Rydberg-like state.

Stampfli and Benemann,[13,14] however, indicated the importance of the polarization effect by a polarizable electropole model and pointed out that the IPs of the spherically symmetric structure of the hydrated Na atom in the surface state strongly decreased with increasing cluster size.

Makov and Nitzan[15] applied a continuum dielectric theory for ions and neutral atomic solutes near planar and spherical (cluster) surfaces and found that the size dependence of the IPs was insensitive to the location of the solute in the cluster. Though their computed asymptotic behavior of the vertical detachment energies of hydrated electron and hydrated I^- ion agreed well with experiment, the observed behavior in the IPs of the Na−water system was unexplainable.

On the other hand, Hashimoto and Morokuma[16−18] reported that surface structures of $Na(H_2O)_n$ where the Na atom was situated on the surface of the water clusters and interior isomers where metal was surrounded by solvent molecules were very

(1) Hart, E. J.; Anbar, M. *The Hydrated Electron*; Wiley: New York, 1970.
(2) Thompson, J. C. *Electrons in Liquid Ammonia*; Oxford University Press: Oxford, U.K., 1976.
(3) Dogonadze, R. R., Kalman, E., Kamyshev, A. A., Ulstrup, J., Eds. *Solvation Phenomena in Specific Physical, Chemical, and Biological Systems*; The Chemical Physics of Solvation, Part C; Elsevier: Amsterdam, 1988.
(4) Hertel, I. V.; Huglin, C.; Nitsch, C.; Schulz, C. P. *Phys. Rev. Lett.* **1991**, *67*, 1767−1770.
(5) Misaizu, F.; Tsukamoto, K.; Sanekata, M.; Fuke, K. *Chem. Phys. Lett.* **1992**, *188*, 241−246.
(6) Takasu, R.; Misaizu, F.; Hashimoto, K.; Fuke, K. *J. Phys. Chem.* **1997**, *A101*, 3078−3087.
(7) Takasu, R.; Hashimoto, K.; Fuke, K. *Chem. Phys. Lett.* **1996**, *258*, 94−100.
(8) Misaizu, F.; Fuke, K.; Hashimoto, K. In *Structures and dynamics of clusters*; Kondow, T., Kaya, K., Terasaki, A., Eds.; Universal Academy Press: Tokyo, 1996; pp 383−388.
(9) Hashimoto, K.; Kamimoto T. In *Structures and dynamics of clusters*; Kondow, T., Kaya, K., Terasaki, A., Eds.; Universal Academy Press: Tokyo, 1996; pp 573−580.
(10) Hashimoto, K.; Kamimoto, T.; Fuke, K. *Chem. Phys. Lett.* **1997**, *266*, 7−15.
(11) Coe, J. V.; Lee, G. H.; Eaton, J. G.; Arnold, S. T.; Sarkas, H. W.; Bowen, K. H.; Ludewigt, C.; Harberland, H.; Worsnop, D. R. *J. Chem. Phys.* **1990**, *92*, 3980−3982.
(12) Barnett, R. N.; Landman, U. *Phys. Rev. Lett.* **1993**, *70*, 1775−1778.
(13) Stampfli, P.; Bennemann, K. H. *Comput. Matter. Sci.* **1994**, *2*, 578−584.
(14) Stampfli, P. *Phys. Rep.* **1995**, *255*, 1−77.
(15) Makov, G.; Nitzan A. *J. Phys. Chem.* **1994,** *98*, 3549−3466.
(16) Hashimoto, K.; He, S.; Morokuma, K. *Chem. Phys. Lett.* **1993**, *206*, 297−306.
(17) Hashimoto, K.; Morokuma, K. *Chem. Phys. Lett.* **1994**, *223*, 423−430.
(18) Hashimoto, K.; Morokuma, K. *J. Am. Chem. Soc.* **1994**, *116*, 11436−11443.

S0002-7863(97)02726-1 CCC: $15.00
Published on Web 04/01/1998

Table 1. Optimized Geometrical Parameters (angstroms and degrees)[a] and Total Binding Energies, $\Delta E(n)$ (kcal/mol), for Potential Minimum Structures of $Li(H_2O)_n$ ($n = 1-2$) Calculated at Various Levels

symbol[b]	level[c]	R_{Li-O1}	θ	R_{Li-O2}	∠O1LiO2	R_{H1-O2}	$\Delta E(n)$[d]
				$Li(H_2O)$			
Ia 1 + 0 (C_{2v})	C	1.917					10.6 (12.2)
Ib 1 + 0 (C_s)	A	1.918	29.3				12.6
	B	1.910	27.1				12.3
				$Li(H_2O)_2$			
IIa 2 + 0 (C_{2v})	B	1.871			174.3		26.8
IIb 2 + 0 (C_2)	C	1.935			107.7		21.1 (25.9)
IIc 2 + 0 (C_s)	B	1.942		1.882	95.5		26.2
IId 2 + 0 (C_1)	A	1.924		1.919	113.0		26.2
IIe 1 + 1 (C_s)	B	1.869				1.774	22.7
	C	1.888				1.883	19.2 (22.4)
IIf 1 + 1 (C_1)	A	1.890				1.778	22.5

[a] Parameters are shown in Figure 1. [b] Corresponds to structures in Figure 1. [c] A: MP2/6-311++G(d,p). B: MP2/6-31++G(d,p). C: HF/6-31++G(d,p). [d] $-\Delta E(n) = E[Li(H_2O)_n] - E[Li] - nE[H_2O]$ (without CPC). Values in parentheses are at MP2/6-31++G(d,p)//HF/6-31++G(d,p).

close in energy by an *ab initio* molecular orbital (MO) method. The calculated IPs of the surface structures having their excess electrons distributed in the surface regions of the clusters were in good agreement with experiment, while those of the interior structures with diffused and delocalized excess electron distribution still decreased for $n \geq 4$.

Despite these efforts, the electronic state of the solvated alkali atom clusters has remained unresolved. In particular, the formation, the structure, and the stability of the two-center state in the small solvent clusters are still controversial. To obtain more insights about the electronic nature of the clusters, it is necessary to carry out a systematic theoretical study of various solvated alkali metals.

In the present paper, we extend our preliminary study of $Li(H_2O)_n$ clusters[19] for $n = 1-8$ by the *ab initio* MO method including electron correlation. We investigate their structures, energetics, and electronic states in detail by comparing them with those of their cation clusters and analyze the cluster-size dependence of their IPs. The questions that we answer are the following: (i) What are the most stable hydration structures of Li atom? Are they similar to those of cation clusters? (ii) What interactions are important in stabilizing $Li(H_2O)_n$? (iii) Do the most stable neutral structures reproduce the peculiar size dependence in the IPs? (iv) Does the electronic state of the neutral clusters change from the one-center atomic state to the two-center ionic state? (v) What is common electronic feature of the hydrated Li and Na?

II. Computational Method

The potential energy surfaces of $Li(H_2O)_n$ ($n = 1-3$) were surveyed, and their stationary points were characterized at the UHF/6-31++G(d,p), UMP2/6-31++G(d,p), and UMP2/6-311++G(d,p) levels.[20] The molecular structures of $Li(H_2O)_n$ with $n = 4-6$ and 8 were optimized, and vibrational analyses were carried out at the UHF/6-31++G(d,p) level using analytic first- and second-derivative techniques. The geometries of $[Li(H_2O)_n]^+$ ($n = 1-6$ and 8) were also optimized at RHF/6-31++G(d,p) level. Single-point MP2 calculations with all electrons active were performed at the HF geometries to assess the effect of electron correlation on the energetics. Ionization potentials were calculated at the MP2/6-31++G(d,p) level. For small complexes with $n \leq 3$, the coupled cluster method using both single and double substitution from the Hartree−Fock determinant (CCSD) was employed to test the reliability of the calculated IP values. The program used was Gaussian-94.[21]

III. Molecular Structure

A. Geometries of Neutral $Li(H_2O)_n$. Figure 1 displays potential minimum structures of $Li(H_2O)_n$ ($n = 1-3$). Tables 1 and 2 show selected optimized geometrical parameters and total binding energies for the structures in Figure 1. The figure and tables including all other structures which have been examined in this study and found to have imaginary frequencies are given in the Supporting Information. In these figure and tables, we use labels of the form **p + q** and molecular symmetry to identify each structure. The values **p** and **q** denote the numbers of water molecules in first and second hydration shells, respectively. The largest eigenvalue of **S** square is 0.7506 among the structures examined, which indicates negligible spin contamination.

The optimized $Li(H_2O)$ structures are **1 + 0** forms (**I*a,b***) in which an H_2O molecule is bound to Li by an oxygen atom. In agreement with previous works,[22−27] the HF method gives a planar structure while correlation makes the structure nonplanar. The energy lowering by the bending is, however, only 0.1 kcal/mol at the MP2/6-311++G(d,p) level, and the bending frequency by the HF/6-31++G(d,p) method is small (124 cm^{-1}). Therefore, $Li(H_2O)$ is mostly stabilized by Li−O bond and very floppy along the bending coordinate. For $Li(H_2O)_2$, **2 + 0** structures (**II*a*−*d***) are more stable than **1 + 1** forms (**II*e,f***) by more than 3.3 kcal/mol at the MP2/6-311++G(d,p) level. Though the molecular symmetry of the stable **2 + 0** structures depends on the level of calculations, the energies of the **2 + 0** forms with different water orientations are close to one another at all levels. The **2 + 0** structures are essentially stabilized by two Li−O bonds. The **1 + 1** structure is slightly deformed from C_s symmetry only at the MP2/6-311++G(d,p) level, but energy lowering by the deformation is nearly zero. The **1 + 1** structures are stabilized by a Li−O bond and a hydrogen bond. The binding energy of a water dimer was calculated to be 6.5 (MP2/6-311++G(d,p)) to 5.0 (HF/6-31++G(d,p)) kcal/mol. The comparison of these values with the data at a higher level of theory (5.58 kcal/mol at MP2/aug-cc-pVTZ[28]) shows that the level of the present treatment is fine, but our values still

(19) Kamimoto, T.; Hashimoto, K. In *Structures and dynamics of clusters*; Kondow, T., Kaya, K., Terasaki, A., Eds.; Universal Academy Press: Tokyo, 1996; pp 563−572.

(20) Hehre, W. J.; Radom, L.; Schleyer, P. v. R.; Pople, J.A. *Ab initio molecular orbital theory*; Wiley: New York, 1986.

(21) Frisch, M. J.; Trucks, G. W.; Schlegel, H. B.; Gill, P. M. W.; Johnson, B. G.; Robb, M. A.; Cheeseman, J. R.; Keith, T.; Petersson, G. A.; Montgomery, J. A.; Raghavachari, K.; Al-Laham, M. A.; Zakrzewski, V. G.; Ortiz, J. V.; Foresman, J. B.; Cioslowski, J.; Stefanov, B. B.; Nanayakkara, A.; Challacombe, M.; Peng, C. Y.; Ayala, P. Y.; Chen, W.; Wong, M. W.; Andres, J. L.; Replogle, E. S.; Gomperts, R.; Martin, R. L.; Fox, D. J.; Binkley, J. S.; Defrees, D. J.; Baker, J.; Stewart, J. P.; Head-Gordon, M.; Gonzalez, C.; Pople. A. *Gaussian 94*; Gaussian, Inc.: Pittsburgh, PA, 1995.

(22) Trenary, M.; Schaefer, H. F.; Kollman, P. *J. Am. Chem. Soc.* **1977**, *99*, 3885−3886.

(23) Trenary, M.; Schaefer, H. F.; Kollman, P. *J. Chem. Phys.* **1978**, *68* , 4047−4050.

(24) Bentley, J.; Carmichael, I. *J. Phys. Chem.* **1981**, *85*, 3821−3826.

(25) Bentley, J. *J. Am. Chem. Soc.* **1982**, *104*, 2754−2759.

(26) Curtiss, L. A.; Pople, J. A. *J. Chem. Phys.* **1985**, *82*, 4230−4235.

(27) Zakharov, I. I.; Avdeev, V. I.; Zhidomirov, G. M. *Surf. Sci.* **1992**, *227*, 407−413.

(28) Xantheas, S. S.; Dunning, T. H., Jr. *J. Chem. Phys.* **1993**, *99*, 8774−8792.

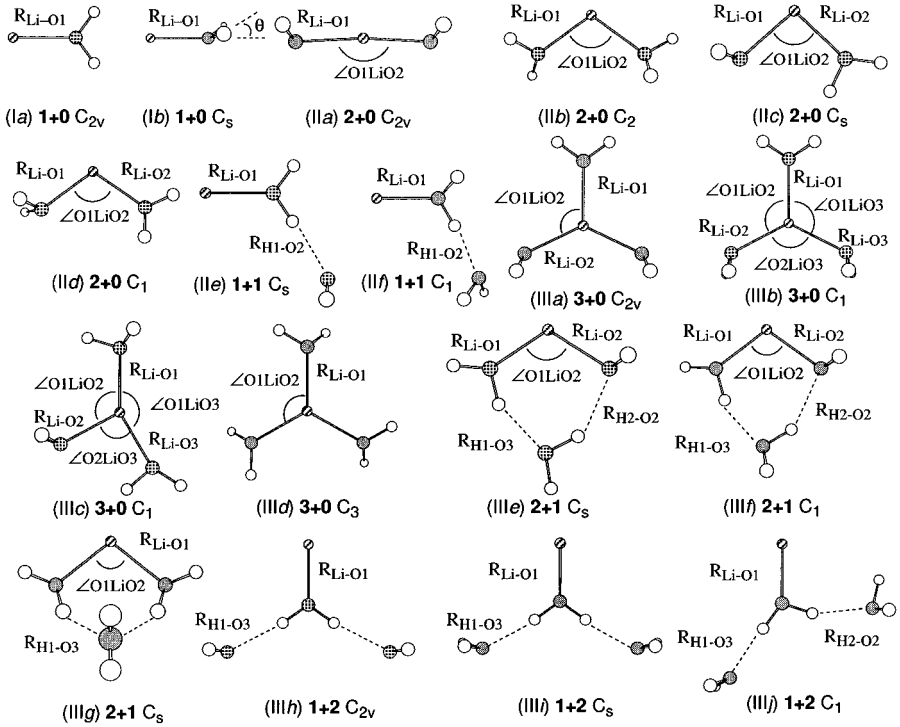

Figure 1. Potential minimum structures of $Li(H_2O)_n$ ($n = 1-3$). Values of selected geometrical parameters and total binding energies without CPC are given Tables 1 and 2.

Table 2. Optimized Geometrical Parameters (angstroms and degrees)[a] and Total Binding Energies, ΔE (kcal/mol), for Potential Minimum Structures of $Li(H_2O)_3$ Calculated at Various Levels

symbol[b]	level[c]	R_{Li-O1}	R_{Li-O2}	R_{Li-O3}	∠O1LiO2	∠O2LiO3	∠O1LiO3	R_{H1-O3}	R_{H2-O2}	ΔE^d
IIIa **3 + 0** (C_{2v})	C	1.915	1.910		115.6					33.2 (42.8)
IIIb **3 + 0** (C_1)	A	1.909	1.913	1.913	117.4	125.3	116.7			42.3
IIIc **3 + 0** (C_1)	B	1.859	1.930	1.860	118.3	92.5	149.2			44.1
IIId **3 + 0** (C_3)	A	1.907			119.6					42.4
	B	1.880			117.5					44.0
	C	1.912			119.9					33.3 (40.2)
IIIe **2 + 1** (C_s)	B	1.850	1.928		113.5			1.796	1.988	40.5
IIIf **2 + 1** (C_1)	A	1.884	1.975		106.6			1.773	2.014	38.3
	C	1.890	2.010		106.0			1.912	2.174	30.1 (39.0)
IIIg **2 + 1** (C_s)	A	1.921			103.2			1.994		36.4
	B	1.888			111.2			1.994		38.2
	C	1.931			99.7			2.126		29.1 (34.7)
IIIh **1 + 2** (C_{2v})	A	1.862						1.829		31.0
	B	1.842						1.825		31.5
	C	1.863						1.929		26.4 (31.2)
IIIi **1 + 2** (C_s)	A	1.863						1.829		31.0
IIIj **1 + 2** (C_1)	B	1.830						1.823	1.844	31.7

[a] Parameters are shown in Figure 1. [b] Corresponds to structures in Figure 1. [c] A: MP2/6-311++G(d,p). B: MP2/6-31++G(d,p). C: HF/6-31++G(d,p). [d] $-\Delta E(n) = E[Li(H_2O)_n] - E[Li] - nE[H_2O]$ (without CPC). Values in parentheses are at MP2/6-31++G(d,p)//HF/6-31++G(d,p).

differ from the experimental value (5.44 ± 0.7 kcal/mol[29]) at most by ~1 kcal/mol. Li−O bond is more important than the hydrogen bond though the interaction between H_2O molecules is stronger in the $Li(H_2O)_2$ than in the pure water dimer. The energy difference between the **2 + 0** and **1 + 1** complexes is larger at the MP2 level than at the HF level. For $Li(H_2O)_3$, the structures having the same **p + q** label are almost isoenergetic with one another, irrespective of water orientation. **3 + 0** structures (**IIIa**−***d***) are the most stable for $n = 3$. **2 + 1** (**IIIe**−***g***) and **1 + 2** (**IIIh**−***j***) isomers are the local minima whose energies are higher than that of **IIId** by more than 4.1 and 11.4 kcal/mol, respectively, at the MP2/6-311++G(d,p) level.

Total binding energies by the MP2/6-31++G(d,p) method are almost identical to our best MP2/6-311++G(d,p) values even at HF geometry for all isomers with $n \leq 3$. The 6-31++G(d,p) basis set is considered to be flexible enough to provide structural trends that are potentially quite valuable. That is, the $Li(H_2O)_n$ clusters are at first stabilized by Li−O interaction and have as many Li−O bonds as possible. On the other hand, the electron correlation does have an effect on the potential surface of the $Li(H_2O)_n$ ($n = 1-3$) though single-point MP2 calculations at HF-optimized geometries with the 6-31++G-(d,p) basis set give a good estimate of total binding energies of the isomers for each n. Therefore, the combination of the HF method for geometry optimization and the MP2 calculation at the HF geometry (MP2//HF) for energetics using the 6-31++G-(d,p) basis set is judged as the appropriate method for larger clusters. In the following sections, we describe total binding energies at the MP2/6-31++G(d,p)//HF/6-31++G(d,p) level unless otherwise mentioned.

The optimized structures and total binding energies of $Li(H_2O)_n$ ($n = 4-6$ and 8) are shown in Figure 2. All of these

(29) Curtiss, L. A.; Frurip, D. L.; Blander, M. *J. Chem. Phys.* **1979**, *71*, 2703−2711.

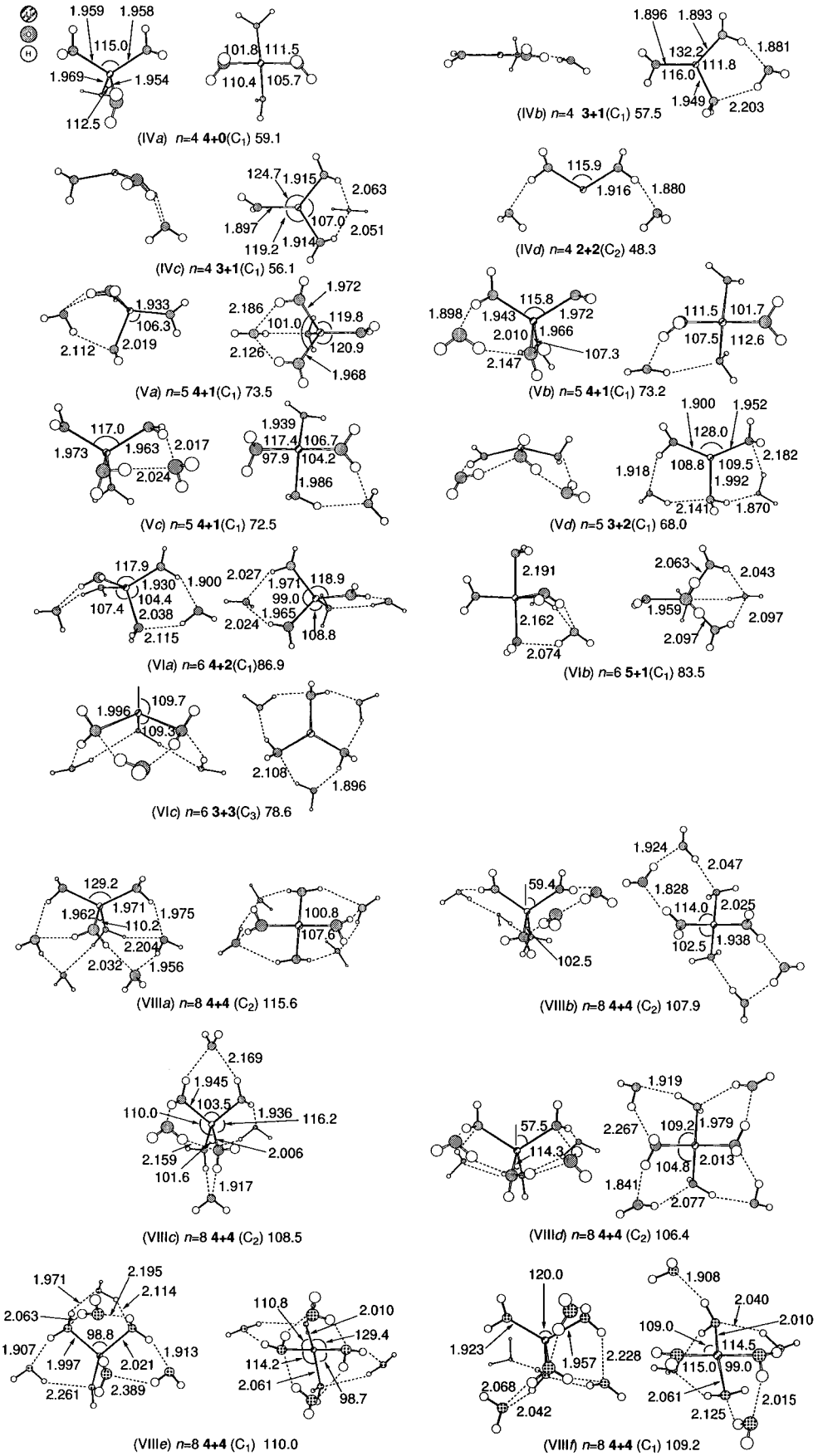

Figure 2. Optimized structures of $Li(H_2O)_n$ (n = 4−6 and 8) calculated at the HF/6-31++G(d,p) level. Geometrical parameters are given in angstroms and degrees. Total binding energies (kcal/mol) without CPC at the MP2/6-31++G(d,p)//HF/6-31++G(d,p) level are also given.

structures have been confirmed to have all real vibrational frequencies. The largest eigenvalue of **S** square is 0.7504 among the optimized $Li(H_2O)_n$ (n = 4−8), which shows the negligible spin contamination as in the case of $n \leq 3$. For $Li(H_2O)_4$, **4** + **0** structure **IV*a***, in which Li atom is surrounded by four H_2O molecules, is the most stable. **3** + **1** structures (**IV*b,c***) where

one H_2O molecule is bound to the **3 + 0** $Li(H_2O)_3$ with different hydrogen-bond orientations and **2 + 2** structure (**IV*d***) are local minima. They are less stable than **IV*a*** by more than 1.6 and 10.8 kcal/mol, respectively. For $Li(H_2O)_5$, we obtained a **5 + 0** structure by a preparatory optimization with the 6-31+G(d) basis set, whose energy was higher than that of the most stable **4 + 1** complex by 3.1 kcal/mol at the MP2/6-31+G(d)//HF/6-31+G(d) level. However, the **5 + 0** structure disappeared with the larger 6-31++G(d,p) basis set converging to the **4 + 1** structure **V*a***. Furthermore, all geometry optimizations with the 6-31++G(d,p) basis set from C_{2v} **5 + 0** complex by following the imaginary normal modes finally reached **4 + 1** forms (**V*a*−*c***). They have different hydrogen-bond orientations from one another but are almost isoenergetic at both MP2//HF and HF levels. **3 + 2** structure **V*d*** is higher in energy than the **4 + 1** structures over 4.5 kcal/mol. With more than five water molecules, the number of potential minimum configurations is very large. Since we found no **5 + 0** structure with the 6-31++G(d,p) basis, we narrowed our focus mainly to **4 + 2** forms for $n = 6$ and found eight **4 + 2,** one **5 + 1,** and one **3 + 3** structure all together. The most stable structure that we have obtained is the **4 + 2** structure **VI*a***, and the eight **4 + 2** structures span a 4.2 kcal/mol range in energy (the high-energy isomers of the **4 + 2** complexes are not shown for brevity). The **5 + 1** and **3 + 3** isomers are less stable than **VI*a*** by 3.4 and 8.3 kcal/mol, respectively.

In the **3 + 3** isomer **VI*c***, the second-shell water molecules donate their OH bonds to bridge the first-shell ligands through hydrogen bonds. It is a member of *3-fold* structure with other **3 + *q*** structures. In the *3-fold* complexes, the O−metal−O angle is much larger than that in the corresponding *surface* Na−water complex[18] with the same *n* due to the strong Li−O bonds. For $Li(H_2O)_8$, we have optimized only **4 + 4** structures (**VIII*a*−*d***). The most stable structure is **VIII*a***, in which two water dimers are bound to $Li(H_2O)_4$ from its lower side. Each water dimer connects three first-shell ligands, and there are eight hydrogen bonds in **VIII*a*** all together. The isomer **VIII*b*** also has two water dimers in the second shell, but each water dimer bridges only two first-shell water molecules. In isomers **VIII*c,d***, four water molecules are bound individually to the **4 + 0** Li-$(H_2O)_4$. These structures, **VIII*b*−*d***, are less stable than **VIII*a*** by more than 7.1 kcal/mol. In search of spherically symmetric isomers, we have tried to optimize an **8 + 0** complex under the D_4 symmetry constraint starting from the structure where eight oxygen atoms are located at corners of a cube. This optimization converged to the structure with long Li−O distances (2.470 Å), and its energy was higher than that of **VIII*a*** by more than 30 kcal/mol (HF). A similar optimization under S_4 symmetry constraint gave the structure with two hydration shells, but it was not a minimum on the potential energy surface. The structures **VIII*e,f*** were obtained by relaxing the S_4 structure along the normal modes for the imaginary frequencies. They were less stable than **VIII*a*** by 5.7 and 6.5 kcal/mol, respectively. The geometrical rearrangement of the second-shell waters forming hydrogen bonds is considered to play an essential role in stabilizing the $Li(H_2O)_8$. As a summary, Li−O interaction is a primarily dominant factor in dictating the structures of Li-$(H_2O)_n$ for $n \leq 4$ and the hydrogen bonds become important in forming a stable asymmetric *interior* structure for larger *n*.

B. Geometries of Cationic $[Li(H_2O)_n]^+$ Clusters. It is interesting to investigate whether the neutral and the corresponding cationic hydration structures of Li are similar to each other. Since the Li−O interaction is much stronger than hydrogen bonds in $[Li(H_2O)_n]^+$, we have optimized mainly their *interior* structures with the maximum number of Li−O bonds. The optimized geometries are shown in Figure 3. All of these structures have been confirmed to have all real harmonic frequencies at the HF/6-31++G(d,p) level.

The structures of $[Li(H_2O)_n]^+$ for $1 \leq n \leq 5$ are similar to those at HF/6-31+G(d) and MP2/aug-cc-pVDZ levels reported by Feller et al.[30,31] Up to four H_2O molecules are bound directly to Li^+ without hydrogen bonds. For $[Li(H_2O)_5]^+$, the **4 + 1** structure **V*a***, where one H_2O molecule is bound to $[Li(H_2O)_4]^+$ via two hydrogen bonds, is more stable than the **5 + 0** isomer **V*b*** by 5.3 kcal/mol. For $[Li(H_2O)_6]^+$, **4 + 2** structures (**VI*a*−*d***) are more stable than the **6 + 0 VI*e*** by more than 5 kcal/mol. It is interesting to notice that the D_{2d} symmetry structure, which is similar to $[Na(H_2O)_6]^+$,[18,32] is slightly lower in energy than the C_2 and C_s symmetry structures found by Feller's group. Though we searched for **5 + 1** structure with C_s symmetry by adding the second-shell water molecule to **V*b***, the optimized structure had an imaginary frequency. The further optimization following the imaginary normal mode converged to the **4 + 2** structure **VI*d***, where a water dimer was located in the second shell. Therefore, we have concluded that the most stable cationic structures for $n \geq 5$ tend to have four water molecules in the first shell, which agrees with the previous reports,[30,31] and optimized only **4 + 4** structures for $n = 8$. The optimized structures of $[Li(H_2O)_8]^+$ are shown in **VIII*a*−*e***. The five structures span about 4 kcal/mol range in energy. Each geometry of **VIII*a*−*d*** was obtained by starting the optimization from the neutral structure with the same label in Figure 2. Thus, these structures are generally similar to the corresponding neutrals. However, several intershell hydrogen bonds are broken in **VIII*b*** and **VIII*c*** cations during the optimization. These complexes have the structures in which two H_2O molecules are bound to the **4 + 2 VI*a***. The complex **VIII*b*** can be also regarded as a structure where two water dimers are bound to the **4 + 0 IV*a***. In addition to these four structures, we searched for an S_4 isomer, starting from the structure where all H_2O molecules were initially located at the corners of a cube without hydrogen bonds, and obtained the structure **VIII*e***. In this structure, all H atoms in the first-shell waters are used in hydrogen bonds and each second-shell water bridges three first-shell waters. Thus, there are 12 hydrogen bonds all together in **VIII*e***.

IV. Energetics

A. Binding Energies and Enthalpies. Total binding energies, $\Delta E(n)$, of both $Li(H_2O)_n$ and $[Li(H_2O)_n]^+$ given in Tables 1 and 2 and Figures 2 and 3 are calculated by

$$-\Delta E(n) = E[M(H_2O)_n] - E[M] - nE[H_2O] \quad (M = Li \text{ and } Li^+) \quad (1)$$

To examine the relative stability of the structural isomers more carefully, we have assessed the basis set super position error (BSSE) for the binding energies by counterpoise correction (CPC). The counterpoise-corrected binding energies and enthalpies (at 1 atm, 298.15 K) of both $Li(H_2O)_n$ and $[Li(H_2O)_n]^+$ are listed in Table 3. Successive binding energies, $\Delta E_{n-1,n}$, and successive binding enthalpies, $\Delta H_{n-1,n}$, of their most stable structures are given in Table 4. For the enthalpies, we used the harmonic vibrational frequencies at the HF/6-31++G(d,p)

(30) Glendening, E. D.; Feller, D. *J. Phys. Chem.* **1995**, *99*, 3060−3067.
(31) Feller, D.; Glendening, E. D.; Kendall, R. A.; Peterson, K. A. *J. Chem. Phys.* **1994**, *100*, 4981−4996.
(32) Kim, J.; Lee, S.; Cho, S. J.; Mhin, B. J.; Kim, K. S. *J. Chem. Phys.* **1995**, *102*, 839−849.

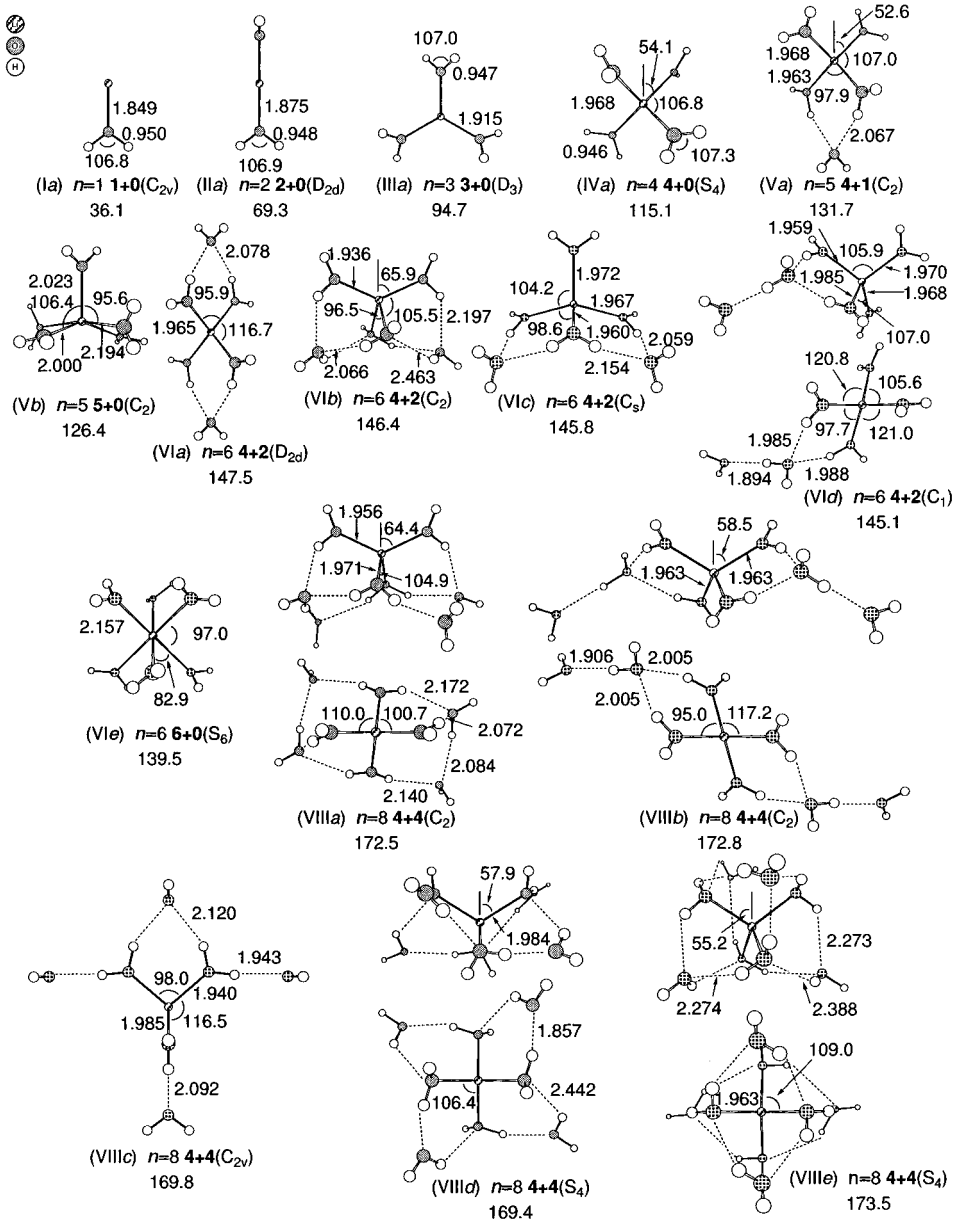

Figure 3. Optimized structures of $[Li(H_2O)_n]^+$ ($n = 1-6$ and 8) calculated at the HF/6-31++G(d,p) level. Geometrical parameters are given in angstroms and degrees. Total binding energies (kcal/mol) without CPC at the MP2/6-31++G(d,p)//HF/6-31++G(d,p) level are also given.

level scaled by 0.895, which was an average ratio between the experimental[33] and calculated frequencies of an isolated H_2O molecule.

The CP estimate should ordinarily be viewed as no better than a semiquantitative correction, but it is useful in examining whether the BSSE's change the relative stability of the isomers seriously. Though BSSE values depend on the structures, the decrease of their binding energies by CPC is within a few kilocalories/mole per water molecule for all neutral isomers. The neutral structure with the maximum number of Li−O bonds is the most stable for each n up through 4, and the *interior* structure having four first-shell ligands is more stable than other isomers for larger n even with CPC. The energy difference between the *interior* and the *3-fold* structures becomes slightly larger as n grows. The $\mathbf{4} + \boldsymbol{q}$ *interior* structure is expected to be more dominant with increasing n for the neutrals. The $Li(H_2O)_n$ is stabilized by 10.0−13.2 kcal/mol in $\Delta E_{n-1,n}$ and 8.1−12.0 kcal/mol in $\Delta H_{n-1,n}$, respectively, by an addition of a water molecule. The relative constancy of $\Delta E_{n-1,n}$ for $Li(H_2O)_n$, at least compared to the sequence for $[Li(H_2O)_n]^+$, indicates a pairwise additive character.

The amount of CPC for $[Li(H_2O)_n]^+$ is comparable with that for the corresponding neutrals. Total binding energies and enthalpies of $[Li(H_2O)_n]^+$ are much greater than the neutrals with the same n as expected from the strong electrostatic interaction. The structures of $[Li(H_2O)_n]^+$ having four first-shell water molecules show greater ΔE_{cpc}, ΔE_{zpc}, and ΔH^{298} than the other isomers where all water molecules are bound directly to Li^+ for $n \geq 5$. Among $\mathbf{4} + \mathbf{2}$ ions, the D_{2d} form is slightly lower in energy than C_2 and C_s forms even with CPC and ZPC. The structure **VIII*b*** shows the largest ΔE_{cpc}, ΔE_{zpc}, and ΔH^{298} values among the $\mathbf{4} + \mathbf{4}$ cations, and the $n = 8$ structures span 5−6 kcal/mol in energy with CPC and ZPC.

Feller et al. have calculated hydration enthalpies of Li^+ at the MP2 level with extended basis sets.[31] Though our basis is not as flexible as theirs, our $\Delta E_{n-1,n}$ and $\Delta H_{n-1,n}$ with CPC are close to their data, and the differences between their values and

(33) Strey, G. *J. Mol. Spectrosc.* **1967**, *24*, 87−99.

Table 3. Counterpoise-Corrected Binding Energies, ΔE_{cpc},[a] and Those with Zero-Point Vibrational Correction, ΔE_{zpc},[a] of $Li(H_2O)_n$ and $[Li(H_2O)_n]^+$ (n = 1−6 and 8) at the MP2/6-31++G(d,p)//HF/6-31++G(d,p) Level[b]

	$Li(H_2O)_n$				$[Li(H_2O)_n]^+$			
n	symbol[c]	ΔE_{cpc}	ΔE_{zpc}	ΔH^{298}	symbol[c]	ΔE_{cpc}	ΔE_{zpc}	ΔH^{298}
1	**I*a* 1 + 0** (C_{2v})	10.0	9.3	8.1	**I*a* 1 + 0** (C_{2v})	33.8	31.9	31.4
2	**II*b* 2 + 0** (C_2)	20.9	18.4	17.5	**II*a* 2 + 0** (D_{2d})	63.5	59.7	59.4
	II*e* 1 + 1 (C_s)	18.2	15.3	14.5				
3	**III*a* 3 + 0** (C_{2v})	34.1	30.2	29.5	**III*a* 3 + 0** (D_3)	86.5	80.8	80.9
	III*d* 3 + 0 (C_3)	34.1	30.1	29.5				
	III*f* 2 + 1 (C_1)	31.0	25.8	25.7				
	III*g* 2 + 1 (C_s)	28.9	23.7	23.5				
	III*h* 1 + 2 (C_{2v})	25.1	20.6	19.7				
4	**IV*a* 4 + 0** (C_1)	46.3	40.4	40.1	**IV*a* 4 + 0** (S_4)	103.2	96.0	96.2
	IV*b* 3 + 1 (C_1)	45.2	38.5	38.8				
	IV*c* 3 + 1 (C_1)	44.1	36.8	37.3				
	IV*d* 2 + 2 (C_2)	39.0	31.9	32.0				
5	**V*a* 4 + 1** (C_1)	57.6	48.5	49.4	**V*a* 4 + 1** (C_2)	117.1	107.3	108.2
	V*b* 4 + 1 (C_1)	57.6	48.7	49.4	**V*b* 5 + 0** (C_2)	111.7	103.1	103.3
	V*c* 4 + 1 (C_1)	56.8	47.6	48.4				
	V*d* 3 + 2 (C_1)	53.2	43.6	44.7				
6	**VI*a* 4 + 2** (C_1)	68.4	56.9	58.3	**VI*a* 4 + 2** (D_{2d})	130.3	118.0	119.5
	VI*b* 5 + 1 (C_1)	64.8	53.5	54.9	**VI*b* 4 + 2** (C_2)	127.4	114.3	116.4
	VI*c* 3 + 3 (C_3)	60.8	48.2	50.0	**VI*c* 4 + 2** (C_s)	128.8	116.7	118.1
					VI*d* 4 + 2 (C_1)	128.3	116.5	117.6
					VI*e* 6 + 0 (S_6)	120.8	109.8	110.7
8	**VIII*a* 4 + 4** (C_2)	90.8	73.5	76.7	**VIII*a* 4 + 4** (C_2)	149.7	132.8	135.3
	VIII*b* 4 + 4 (C_2)	84.8	68.8	71.0	**VIII*b* 4 + 4** (C_2)	151.4	135.5	137.2
	VIII*c* 4 + 4 (C_2)	84.0	67.6	70.1	**VIII*c* 4 + 4** (C_{2v})	148.7	133.6	134.8
	VIII*d* 4 + 4 (C_2)	81.6	64.7	67.5	**VIII*d* 4 + 4** (S_4)	146.2	129.9	132.1
	VIII*e* 4 + 4 (C_1)	84.8	68.3	70.9	**VIII*e* 4 + 4** (S_4)	150.7	132.8	136.0
	VIII*f* 4 + 4 (C_1)	84.5	68.1	70.6				

[a] Harmonic vibrational frequencies at the HF/6-31++G(d,p) level were scaled by 0.895 and used. [b] Counterpoise-corrected enthalpies at 1 atm and 298.15 K, ΔH^{298},[a] are also presented. Values are given in kcal/mol. [c] Indicates the structures in Figures 1−3.

Table 4. Successive Binding Energies, $\Delta E_{n-1,n}$,[a] and Successive Binding Enthalpies, $\Delta H_{n-1,n}$[b] (1 atm, 298.15 K), of the Most Stable Structures of $[Li(H_2O)_n]$ and $[Li(H_2O)_n]^+$ (n = 1−6) in kcal/mol

	$[Li(H_2O)_n]$		$[Li(H_2O)_n]^+$					
	MP2/6-31++G(d,p)// HF/6-31++G(d,p) (this work)[c]		MP2/6-31++G(d,p)// HF/6-31++G(d,p) (this work)[c]		MP2/aug-cc-pVDZ// MP2/aug-cc-pVDZ (ref 31)[d]		expt (ref 34)	expt (ref 35)
n	$\Delta E_{n-1,n}$	$\Delta H_{n-1,n}$	$\Delta E_{n-1,n}$	$\Delta H_{n-1,n}$	$\Delta E_{n-1,n}$	$\Delta H_{n-1,n}$	$\Delta H_{n-1,n}$	$\Delta H_{n-1,n}$
1	10.0	8.1	33.8	31.4	33.2	32.2	34.0[f]	32.7
2	10.9	9.4	29.7	28.0	29.3	27.5	25.8	27.2
3	13.2	12.0	23.1	21.5	22.8	21.7	20.7	22.3
4	12.2	10.6	16.7	15.3	17.5	16.1	16.4	17.0
5	11.3	9.3	13.9	12.0	15.0	13.1	13.9	14.3
6	10.8	8.9	13.1	11.3	12.1	10.4[e]	12.1	15.1

[a] $-\Delta E_{n-1,n} = E([M(H_2O)_n]^+) - E([M(H_2O)_{n-1}]^+) - E(H_2O)$. [b] $-\Delta H_{n-1,n} = H([M(H_2O)_n]^+) - H([M(H_2O)_{n-1}]^+) - H(H_2O)$. Harmonic vibrational frequencies at HF/6-31++G(d,p) level scaled by 0.895 were used. [c] Counterpoise corrected. [d] With frozen core approximation. [e] At MP2/aug-cc-pVDZ//HF/cc-pVDZ level. [f] Extrapolated value.

ours are at most ∼1 kcal/mol for all n. Dzidic and Kebarle[34] have reported the successive enthalpy change for $[Li(H_2O)_2]^+$ through $[Li(H_2O)_6]^+$ and extrapolated them backward to arrive at their value for $[Li(H_2O)]^+$. Very recently, Rodgers and Armentrout[35] have determined bond dissociation energies of $[Li(H_2O)_n]^+$ (n = 1−6) directly by kinetic-energy-dependent collision-induced dissociation experiments in a guided ion mass spectrometer. They have reported bond dissociation enthalpies based on theoretical structures and vibrational frequencies[31] (see Table 4). The present result agrees well with these experimental ones for each n. $\Delta E_{n-1,n}$ and $\Delta H_{n-1,n}$ decrease greatly from n = 1−4 mainly due to the progressive saturation in bonding properties of Li^+. Their values for $n \geq 5$ become smaller than those for $n = 4$, reflecting the formation of the first shell at n = 4.

B. Energy Decomposition Analysis. From the cluster-size (n) dependence of the energetics, we notice that the total binding energies for the most stable neutral structures are almost additive against n even after the first shell has been completed. To obtain more insights about the energetics, it is instructive to divide the total hydration energy into the contribution of interaction among waters, $\Delta E_S(n)$, and that of solute−water cluster interaction, $\Delta E_M(n)$. According to the previous work,[18] we define the $\Delta E_S(n)$ and $\Delta E_M(n)$ by the following formulas 2 and 3, respectively.

$$-\Delta E_S(n) = E[(H_2O)_n^{\#}] - nE[H_2O] \quad (2)$$

$$-\Delta E_M(n) = E[M(H_2O)_n] - E(M) - E[(H_2O)_n^{\#}] \quad (M = Li \text{ and } Li^+) \quad (3)$$

Here, $E[(H_2O)_n^{\#}]$ is the energy of a complex of n H_2O molecules whose structure is fixed at that of the $Li(H_2O)_n$ or $[Li(H_2O)_n]^+$ cluster in question. $\Delta E_S(n)$ gives the interaction energy among the H_2O molecules in the hydrated Li or Li^+ complex. The $\Delta E_M(n)$ is the interaction energy between the prepared $(H_2O)_n^{\#}$ cluster and the Li atom or ion, and the sum of the two components gives the total binding energy $\Delta E(n)$:

(34) Dzidic, I.; Kebarle, P. *J. Phys. Chem.* **1970**, *74*, 1466−1474.
(35) Rodgers, M. T.; Armentrout, P. B. *J. Phys. Chem.* **1997**, *A101*, 1238−1249.

$$\Delta E(n) = \Delta E_S(n) + \Delta E_M(n) \quad (4)$$

The values of $\Delta E(n)$, $\Delta E_S(n)$, and $\Delta E_M(n)$ for both neutral and ionic complexes are listed in Table 5. In the most stable neutral structures, $\Delta E_M(n)$ is a main contributor of the total binding energy for all n. $\Delta E_S(n)$ is nearly zero or negative for $n \leq 4$ and is positive for larger n. This fact indicates that stabilization energies are gained by the Li−O bond formation overcoming the repulsion among the water molecules in the $n \leq 4$ clusters and the hydrogen-bond interaction becomes important after the first shell is formed.

It is interesting to notice that $\Delta E_M(n)$ still increases for $n \geq 5$ though the slope becomes smaller than that for $n \leq 4$. It corresponds to the growth of the second hydration shell for $n \geq 5$. To analyze the situation more clearly, we further divide the binding energy for $n \geq 4$ by the following formulas 5 and 6.

$$\Delta E_S(n) = \Delta E(W_4^{\#}{}_{1st}) + \Delta E(W_q^{\#}{}_{2nd}) + \Delta E(W_4^{\#}{}_{1st}\text{-}W_q^{\#}{}_{2nd}) \quad (5)$$

$$\Delta E_M(n) = \Delta E(Li{-}W_4^{\#}{}_{1st}) + \Delta E(Li{-}W_q^{\#}{}_{2nd}) + \Delta E(Li{-}W_4^{\#}{}_{1st}{-}W_q^{\#}{}_{2nd}) \quad (6)$$

In this analysis, we regard the $\mathbf{4} + \boldsymbol{q}$ $Li(H_2O)_n$ as a complex consisting of three parts: a Li atom, the first-shell $(H_2O)_4$ cluster, and the second-shell $(H_2O)_q$ cluster. $-\Delta E(W_4^{\#}{}_{1st})$ and $-\Delta E(W_q^{\#}{}_{2nd})$ are the energies of the $(H_2O)_4^{\#}$ and the $(H_2O)_q^{\#}$ relative to the isolated water molecules. $\Delta E(W_4^{\#}{}_{1st})$ includes all intrashell interactions among the first-shell waters and $\Delta E(W_q^{\#}{}_{2nd})$ those among the second-shell ligands. $\Delta E(W_4^{\#}{}_{1st})$ and $\Delta E(W_q^{\#}{}_{2nd})$ also include the deformation energy of each water monomer from a free H_2O molecule. $\Delta E(W_4^{\#}{}_{1st}{-}W_q^{\#}{}_{2nd})$ is the interaction energy between the first-shell $(H_2O)_4$ and the second-shell $(H_2O)_q$ and includes all intershell interactions among water monomers up to $\mathbf{4} + \boldsymbol{q}$ body term. On the other hand, $\Delta E(Li{-}W_4^{\#}{}_{1st})$ is the interaction energy between Li and the first-shell $(H_2O)_4$ cluster and $\Delta E(Li{-}W_q^{\#}{}_{2nd})$ is that between Li and the second-shell $(H_2O)_q$ cluster. In other words, $\Delta E(Li{-}W_4^{\#}{}_{1st})$ is the sum of all interactions among Li and the first-shell waters up to five body terms and $\Delta E(Li{-}W_q^{\#}{}_{2nd})$ is that among the Li atom and the second-shell molecules up to $\boldsymbol{q} + \mathbf{1}$ body terms. Therefore, $\Delta E(Li{-}W_4^{\#}{}_{1st}{-}W_q^{\#}{}_{2nd})$ is the overall intershell interaction energy among Li, the first-shell and the second-shell waters including up to $\mathbf{5} + \boldsymbol{q}$ body terms. We call $\Delta E(Li{-}W_4^{\#}{}_{1st}{-}W_q^{\#}{}_{2nd})$ the *intershell Li−water interaction* energy in the following discussion. The values for each term in eqs 5 and 6 are summarized in Table 6.

First of all, we look at the results for the most stable neutral structures for each n (**IV*a***, **V*a***, **VI*a***, and **VIII*a***). In these clusters, $\Delta E(Li{-}W_4^{\#}{}_{1st})$ is a main contributor in $\Delta E_M(n)$, while $\Delta E(Li{-}W_q^{\#}{}_{2nd})$ shows almost zero contribution. $\Delta E(Li{-}W_4^{\#}{}_{1st})$ changes only slightly from the **IV*a*** to the **VIII*a***, indicating that the growth of the second shell does not affect the local interaction between Li and the four first-shell water molecules very much. On the other hand, $\Delta E(Li{-}W_4^{\#}{}_{1st}{-}W_q^{\#}{}_{2nd})$ becomes larger as n grows and this *intershell Li−water interaction* is mainly responsible to the increase of the $\Delta E_M(n)$. It becomes more than 25% of total $\Delta E_M(8)$ and the second important contributor of the total binding energy for the **VIII*a***. The change of $\Delta E(W_4^{\#}{}_{1st})$ from the **IV*a*** to the **VIII*a*** is about 1 kcal/mol per H_2O molecule, which also indicates little effect of the second-shell waters on the core $Li(H_2O)_4$. The interaction energy among the second-shell water molecules is almost zero for $n = 5$ and 6 but becomes about double the hydrogen-bond energy of a water dimer in the **VIII*a***. This is consistent with its structure where two water dimers are located individually in the second shell. $\Delta E(W_4^{\#}{}_{1st}{-}W_q^{\#}{}_{2nd})$ increases as n grows but is 20.0 kcal/mol for the **VIII*a***. As a result, the $\Delta E(Li{-}W_4^{\#}{}_{1st}{-}W_q^{\#}{}_{2nd})$ becomes greater than the $\Delta E(W_4^{\#}{}_{1st}{-}W_q^{\#}{}_{2nd})$ for this complex. The result of higher energy isomers for $n = 5$ is similar to that of **V*a***. Their difference is mainly seen in $\Delta E(W_4^{\#}{}_{1st}{-}W_q^{\#}{}_{2nd})$, reflecting the different hydrogen bonds between the first- and second-shell water molecules. On the other hand, in high-energy isomers for $n = 8$, $\Delta E(Li{-}W_4^{\#}{}_{1st})$ is a little smaller than that of **VIII*a*** and $\Delta E(W_4^{\#}{}_{1st}{-}W_q^{\#}{}_{2nd})$ is the second greatest contributor to the total binding energy. Thus, the interaction between the Li and the first-shell ligands and that among the water molecules are important factors but the *intershell Li−water interaction* becomes essential in forming the most stable structures for $n \geq 5$, especially for $n = 8$.

Table 5. Contributions of Interaction among Waters, $\Delta E_S(n)$,[a] and Solute−Water Cluster Interaction, $\Delta E_M(n)$,[a] in Total Binding Energies of the Most Stable $[Li(H_2O)_n]$ and $[Li(H_2O)_n]^+$ ($n = 1{-}6$ and 8) at the MP2/6-31++G(d,p)//HF/6-31++G(d,p) Level

	$Li(H_2O)_n$				$[Li(H_2O)_n]^+$			
n	symbol[b]	$\Delta E(n)$	$\Delta E_S(n)$	$\Delta E_M(n)$	symbol[b]	$\Delta E(n)$	$\Delta E_S(n)$	$\Delta E_M(n)$
1	**I*a***	12.2	0.1	12.1	**I*a***	36.1	0.3	35.8
2	**II*b***	25.9	−1.5	27.4	**II*a***	69.3	−1.3	70.6
3	**III*a***	42.8	−4.7	47.5	**III*a***	94.7	−4.9	99.6
4	**IV*a***	59.1	−8.6	67.7	**IV*a***	115.1	−9.9	125.0
5	**V*a***	73.5	2.5	71.0	**V*a***	131.7	−3.9	135.6
6	**VI*a***	86.9	6.2	80.7	**VI*a***	147.5	0.3	147.2
8	**VIII*a***	115.6	16.4	99.2	**VIII*b***	172.8	14.7	158.1

[a] $\Delta E_S(n)$ and $\Delta E_M(n)$ are defined by eqs 2 and 3. $\Delta E_S(n) + \Delta E_M(n)$ is equal to $\Delta E(n)$. See text. Values are without CPC and given in kcal/mol. [b] Indicates structures in Figures 1−3.

The same analysis has been carried out for the hydrated Li^+ clusters. Total binding energies of the *interior* ion complexes also show a monotonic increase with n, and the slope is much larger than in the neutral complex. This reflects the strong electrostatic interaction between the Li^+ and solvent water molecules as seen in the large $\Delta E(Li{-}W_4^{\#}{}_{1st})$ and $\Delta E(Li{-}W_q^{\#}{}_{2nd})$ values in Table 6. The direct Li^+−water cluster interaction is important even for the second-shell H_2O molecules. The interaction among the first-shell waters is repulsive, and that among the second-shell waters reflects the structural feature of the clusters as in the case of the neutrals. $\Delta E(W_4^{\#}{}_{1st}{-}W_q^{\#}{}_{2nd})$ values for **VIII*b*−*d*** cations are smaller than those for the corresponding neutral clusters. This is consistent with the facts that **VIII*b,c*** have fewer intershell hydrogen bonds than their corresponding neutrals and that the intershell hydrogen bonds in **VIII*d*** are longer than those in its neutral form. Note that our $\Delta E(W_4^{\#}{}_{1st}{-}W_q^{\#}{}_{2nd})$ contains neither the polarization nor the charge transfer induced by the presence of Li^+. If we estimate the interaction energies between the perturbed $W_4^{\#}{}_{1st}$ and $W_q^{\#}{}_{2nd}$ of the most stable structures by treating Li^+ as a point charge, they are 8.2 (**V*a***), 16.0 (**VI*a***), and 20.0 (**VIII*b***) kcal/mol, respectively. Thus, although the perturbation by Li^+ increases the first-shell−second-shell water interaction energies, the change in $\Delta E(W_4^{\#}{}_{1st}{-}W_q^{\#}{}_{2nd})$ is at most 0.8−0.9 kcal/mol per second-shell H_2O molecule. Interestingly, $\Delta E(Li{-}W_4^{\#}{}_{1st}{-}W_q^{\#}{}_{2nd})$ in cations is small or negative even at $n = 8$, which is in sharp contrast to the neutral $Li(H_2O)_n$. Therefore, the electrostatic interactions between Li^+ and water molecules as well as the intershell interactions among waters via hydrogen bonds play an important role in the total binding energy of $[Li(H_2O)_n]^+$, while the *intershell Li−water interaction* is not essential in stabilizing the cation complexes.

Table 6. Detailed Components[a] of Interaction between Solute and Water Cluster, $\Delta E_M(n)$, and That among Waters, $\Delta E_S(n)$, of **4** + ***q*** Type $Li(H_2O)_n$ and $[Li(H_2O)_n]^+$ ($n \geq 4$) at the MP2/6-31++G(d,p)//HF/6-31++G(d,p) Level

			$\Delta E_M(n)$			$\Delta E_S(n)$		
n	**4** + **q**	symbol[b]	$\Delta E(Li-W_4^{\#}{}_{1st})$	$\Delta E(Li-W_q^{\#}{}_{2nd})$	$\Delta E(Li-W_4^{\#}{}_{1st}-W_q^{\#}{}_{2nd})$	$\Delta E(W_4^{\#}{}_{1st})$	$\Delta E(W_q^{\#}{}_{2nd})$	$\Delta E(W_4^{\#}{}_{1st}-W_q^{\#}{}_{2nd})$
					$Li(H_2O)_n$			
4	**4** + **0**	**IV*a***	67.7	0.0	0.0	−8.6	0.0	0.0
5	**4** + **1**	**V*a***	66.5	0.6	3.9	−10.4	0.2	12.7
	4 + **1**	**V*b***	67.1	0.3	4.0	−8.1	0.1	9.8
	4 + **1**	**V*c***	68.1	1.2	5.2	−9.3	0.3	7.0
6	**4** + **2**	**VI*a***	68.5	1.3	10.9	−10.6	0.2	16.6
8	**4** + **4**	**VIII*a***	69.2	2.3	27.7	−12.7	9.1	20.0
	4 + **4**	**VIII*b***	64.4	2.3	9.0	−7.6	11.6	28.2
	4 + **4**	**VIII*c***	64.2	1.6	16.4	−8.6	0.4	34.4
	4 + **4**	**VIII*d***	61.5	−0.6	4.3	−4.0	3.1	42.2
	4 + **4**	**VIII*e***	60.7	1.7	8.9	−5.2	1.8	42.0
	4 + **4**	**VIII*f***	63.5	1.9	16.3	−8.2	0.7	34.9
					$[Li(H_2O)_n]^+$			
4	**4** + **0**	**IV*a***	125.0	0.0	0.0	−9.9	0.0	0.0
5	**4** + **1**	**V*a***	124.3	10.8	0.6	−11.5	0.2	7.4
6	**4** + **2**	**VI*a***	124.8	20.9	1.5	−14.1	0.0	14.3
	4 + **2**	**VI*b***	116.8	18.8	−4.3	−8.4	0.7	22.8
	4 + **2**	**VI*c***	123.1	21.1	0.8	−13.1	−0.3	14.3
	4 + **2**	**VI*d***	123.9	16.4	0.9	−11.5	6.2	9.3
8	**4** + **4**	**VIII*a***	120.8	35.7	−1.9	−14.4	9.8	22.4
	4 + **4**	**VIII*b***	124.5	31.4	2.2	−14.5	11.8	17.5
	4 + **4**	**VIII*c***	124.8	35.4	4.3	−13.9	−2.2	21.5
	4 + **4**	**VIII*d***	116.3	23.9	−1.9	−4.9	2.3	33.7
	4 + **4**	**VIII*e***	108.3	38.6	−12.0	−5.6	1.5	42.8

[a] Definition of components are given by eqs 2 and 3. See text. Values are without CPC and given in kcal/mol. [b] Indicates the structures in Figures 2 and 3.

Table 7. Vertical and Adiabatic Ionization Potentials (eV) of the Most Stable Structures[a] of $Li(H_2O)_n$ ($n = 1-6$ and 8) Calculated at HF-Optimized Geometries with 6-31++G(d,p) Basis Set[b]

n	**p** + **q** (sym)	label[c]	MP2//HF	MP2(FC)[d] //HF	CCSD(FC)[d] //HF	expt (ref 6)
0	**0** + **0**		5.34 (5.34)	5.33 (5.33)	5.33	5.39
1	**1** + **0**	**I*a***	4.32 (4.30)	4.32 (4.31)	4.34	4.41
2	**2** + **0**	**II*b***	3.71 (3.45)	3.71 (3.48)	3.74	3.80
3	**3** + **0**	**III*a***	3.22 (3.09)	3.22 (3.08)	3.24	3.37
4	**4** + **0**	**IV*a***	3.05 (2.91)	3.05 (2.89)	—	3.14
5	**4** + **1**	**V*a***	3.12 (2.81)	3.11 (2.80)	—	3.12
6	**4** + **2**	**VI*a***	3.17 (2.71)	3.17 (2.69)	—	3.12
8	**4** + **4**	**VIII*a***	3.11 (2.86)	3.11 (2.83)	—	—

[a] The most stable structures with CPC and ZPC for each *n* were used. [b] Adiabatic IPs are given in parentheses. [c] Indicates structures in Figures 1 and 2. [d] Frozen core approximation was employed.

V. Ionization Potentials and Electronic State of $Li(H_2O)_n$ ($0 \leq n \leq 8$)

The calculated ionization potentials (IPs) of the most stable $Li(H_2O)_n$ clusters are presented in Table 7. For $0 \leq n \leq 3$, we calculated the vertical IPs by both MP2 and CCSD methods and found that the values by these two methods were very close to each other for all *n*. The results by MP2/6-31++G(d,p) with and without frozen core approximation are almost identical to each other. We discuss the IPs at the MP2/6-31++G(d,p)//HF/6-31++G(d,p) level. Adiabatic IPs are smaller than vertical ones particularly for $n \geq 4$ because of the structural relaxation from the neutrals to the cations.

The calculated vertical IPs of the most stable *interior* complexes, which correspond to the threshold energies measured by the photoionization, are in good agreement with a recent experiment.[6] They decrease monotonically until $n = 4$ and become nearly constant for larger *n* converging to the bulk limit of the vertical detachment energies (VDEs) of $(H_2O)_n^-$ (3.2 eV).[11] The total gross population in Li s basis functions, which is given in the Supporting Information, shows that the population in the inner and outer valence s functions on Li decreases rapidly as *n* grows and becomes nearly constant, being 0.3−0.4 e for $n \geq 4$. On the other hand, the population in the diffuse function increases gradually until $n = 4$ and decreases slightly with further hydration. As a result, the Li valence s atomic orbital holds 0.7 ($n = 4$) to 0.5 ($n = 8$) e total in clusters with $n \geq 4$. Thus, the character of the odd electron changes from the normal valence electron to the diffused hydrated electron during the first-shell formation, and the second-shell waters are considered to share the excess electron squeezed out of the first shell.

Figure 4 represents the difference in the electron density between the neutral and the cationic $Li(H_2O)_n$ at the neutral geometries. This figure shows the spatial distribution of the excess electron being ejected by the photoionization. The excess electron density is distributed around both the Li atom and H_2O molecules in $Li(H_2O)_2$. The excess electron distribution around Li is in the space opposite to the H_2O molecules rather than that between the Li and O atoms. In $Li(H_2O)_4$, the excess electron is separated from Li and distributed in the space on and between H_2O molecules. In $Li(H_2O)_6$, we see the electron distribution not in the vicinity of Li but in the space between the first- and the second-shell H_2O molecules and on H_2O molecules. In $Li(H_2O)_8$, the excess electron is mainly distributed in the space on and between the second-shell H_2O molecules being expelled from the first-shell cavity rather than the space on the first-shell waters. Therefore, the electronic nature of the hydrated Li atom clusters changes as *n* grows from the one-center atomic state for $n \leq 3$ to the two-center ionic state for $n \geq 4$ with a gradual localization of the excess electron. The valence electron is separated from Li and becomes distributed outside the first-shell cavity by the stepwise hydration. In other words, the excess electron is considered to be ejected by the photoionization not from around Li atom but from the water molecules for $n \geq 4$. It is worth noticing that two second-shell H_2O molecules for $n = 8$ point their free OH bonds toward the excess electron in the surface region of the cluster. The two dangling hydrogens do not take part in the hydrogen bonds but interact with the excess electron. These electrophilic hydrogens act as actuators of the surface state. This situation is similar to the surface state of the negatively charged small- and medium-

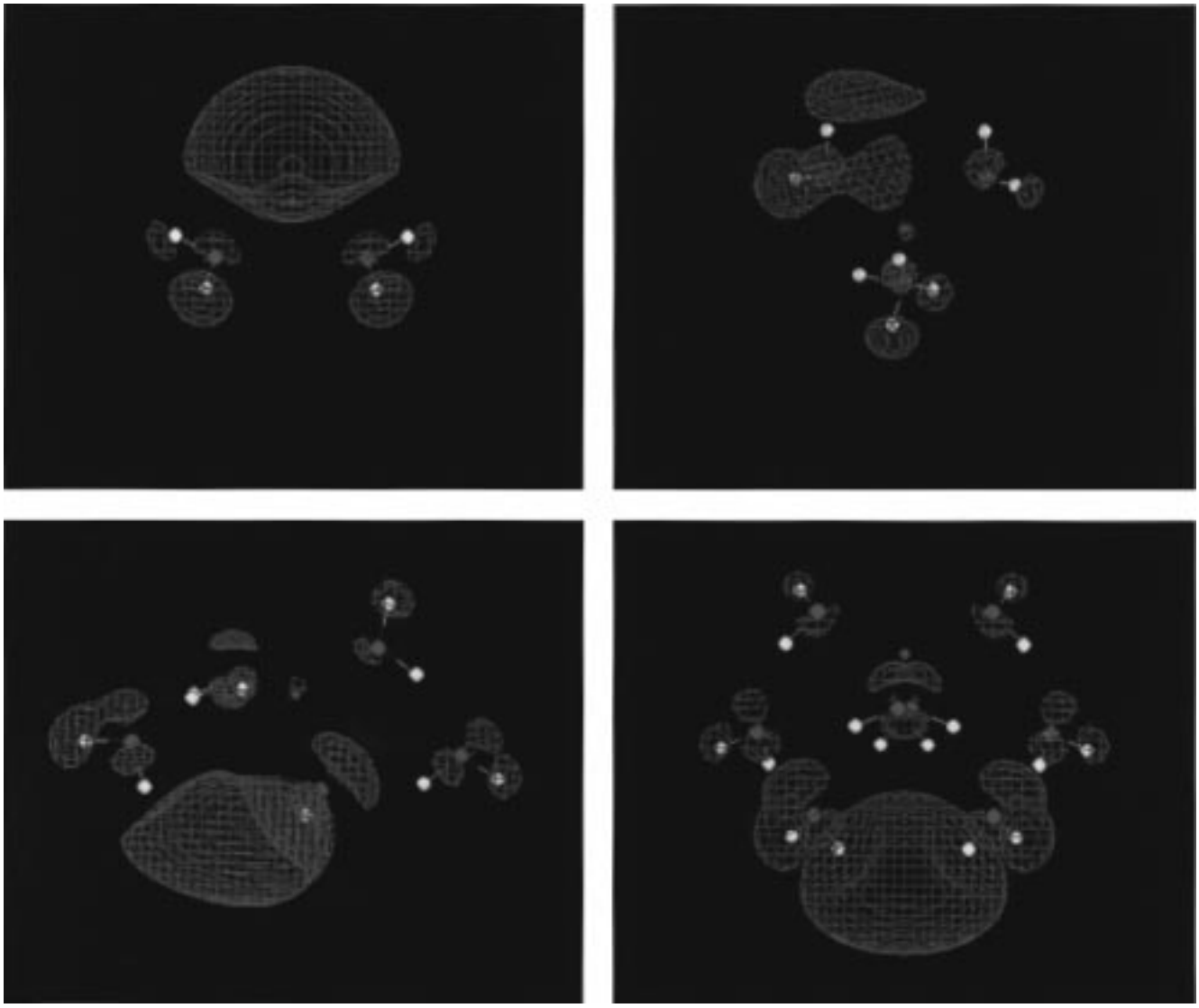

Figure 4. Contour surface of excess electron density for $Li(H_2O)_n$ (n = 2, 4, 6, and 8) calculated at the MP2/6-31++G(d,p) level. Li, O, and H atoms are shown by orange, red, and white balls, respectively. The electron density of blue surface is 0.001 e/Bohr^3. Top left: for n = 2 complex, **II*b***, in Figure 1. Top right: for n = 4 complex, **IV*a***, in Figure 2. Bottom left: for n = 6 complex, **VI*a***, in Figure 2. Bottom right: for n = 8 complex, **VIII*a***, in Figure 2.

sized water clusters observed by the *ab initio* MO[36,37] and the quantum path-integral[38] methods.

To discuss the electronic state of the clusters in more detail, we constructed model clusters by replacing the Li atom by a point charge in $Li(H_2O)_n$. The total charge of the model clusters was kept neutral. Consequently, the model clusters can be regarded as the negatively charged $(H_2O)_n$ clusters interacting with a cation center, whose water geometry is fixed at that in the corresponding $Li(H_2O)_n$. Vertical IPs (VIPs) of $Li(H_2O)_n$ and those of model clusters[39] as functions of n are shown in Figure 5a. The VIPs of the model clusters almost coincide with those of the true Li−water complexes for $n \geq 4$. In addition, the excess electron distribution of the model cluster (not shown for brevity) is similar to that of the corresponding true Li−water cluster with the same $n \geq 4$. These facts indicate that Li in the hydration systems releases its valence electron and act as a cation center with more than four water molecules. The similarity in the first-shell structure between the neutral and cationic $Li(H_2O)_n$ ($n \geq 4$) is considered to result from this electronic nature of the neutrals. Once the neutral clusters become $[Li(H_2O)_4]^+$ interacting with the hydrated electron and the expelled electron starts localization in the water clusters, their IPs behave insensitively to the cluster size (n).

Barnett and Landman reported that the reduced variation of IPs for $Na(H_2O)_n$ ($n \geq 4$) reflected the formation of a molecular shell about Na by the LSD calculation. The electronic state they found for $Na(H_2O)_n$ for $n \geq 4$ was the surface Rydberg-like state where the electron was delocalized and spread rather equally about the water molecules. Their result for Na−water clusters and ours for Li−water systems are different in the electron localization but similar to each other in such a sense that the excess electron is distributed in the surface region of the clusters.

The calculated IPs of the *surface* complex of $Na(H_2O)_n$ whose structure resembled that of the *3-fold* $Li(H_2O)_n$, agreed well with

(36) Kim, K. S.; Park, I.; Lee, S.; Cho, K.; Lee, J. Y.; Kim, J.; Joannopoulos, J. D. *Phys. Rev. Lett.* **1996**, *76*, 956−959.

(37) Lee, S.; Lee, S. J.; Lee, J. Y.; Kim, J.; Kim, K. S.; Park, I.; Cho, K.; Joannopoulos, J. D. *Chem. Phys. Lett.* **1996**, *254*, 128−134.

(38) Barnett, R. N.; Landman, U.; Cleveland, C. L. *J. Chem. Phys.* **1988**, *88*, 4429−4447.

(39) We placed the Li basis set on the cation center in the n = 8 model cluster since the SCF without the basis converged not to the surface state but to the internal state.

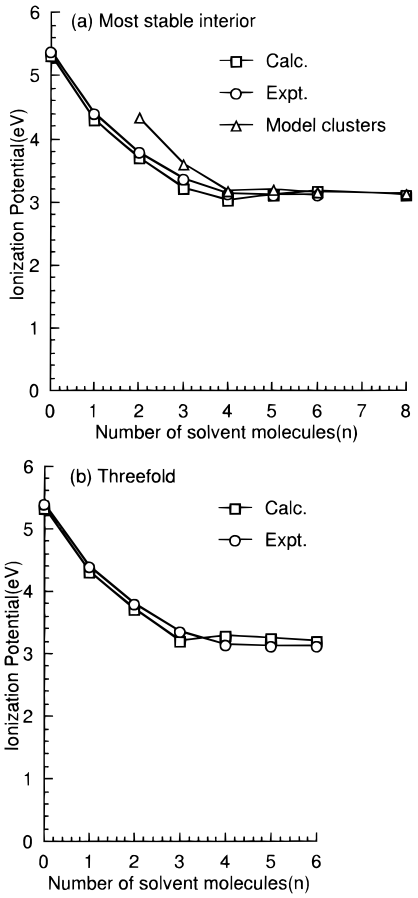

Figure 5. (a) Vertical ionization potentials (eV) of the most stable $Li(H_2O)_n$ ($n = 1-6$ and 8) as a function of n at the MP2/6-31++G(d,p)//HF/6-31++G(d,p) level together with the experimental result. Values for model clusters are also plotted (see text). (b) Vertical ionization potentials (eV) of *3-fold* $Li(H_2O)_n$ ($n = 1-6$) as a function of n at the MP2/6-31++G(d,P)//HF/6-31++G(d,p) level together with the experimental result.

the experiment, and they were also almost constant (~3.2 eV) for $n \geq 4$.[17] The VIPs for *3-fold* complexes are plotted against n together with the experimental result in Figure 5b. Though the *3-fold* complexes are high energy isomers for $n \geq 4$ and thus their VIPs may not be observed in the photoionization experiment, their size dependence in VIPs is close to that of the most stable *interior* structure and the experiment. In both *3-fold* $Li(H_2O)_n$ and *surface* $Na(H_2O)_n$, only three or four water molecules interact with the metal. And the excess electron distributions in the *3-fold* $Li(H_2O)_n$ and the *surface* $Na(H_2O)_n$ with the same n are similar to each other. They are rather localized around metals in the surface region of the clusters and extend widely in space in the directions where hydrating H_2O molecules do not exist. In addition, they are almost unchanged for $n \geq 4$. The indirect hydration in the second and further shell does not very much affect the local electronic state around the metal. Therefore, the IPs of these complexes remain nearly constant around $n = \sim 4$. Though the reason IPs of the *3-fold* $Li(H_2O)_n$ and the *surface* $Na(H_2O)_n$ with $n \geq 4$ coincide with the VDE of $(H_2O)_n^-$ needs more elaborated investigation, we can say that these two kinds of clusters and the most stable *interior* $Li(H_2O)_n$ are all surface state, in which the excess electron is rather localized in the part of cluster surface. The surface ionization is expected to take place in these clusters.

VI. Conclusions

In the present study, we have investigated neutral and cationic $Li(H_2O)_n$ ($n = 1-6$ and 8) by an *ab initio* MO method, including the electron correlation, and reached the following conclusions:

(1) The interior structure with four H_2O molecules around Li in the first shell and more in the second shell is the most stable for $n \geq 4$ for both neutral and cationic hydrated Li clusters. Li−O interactions play an essential role in dictating the molecular structures for $1 \leq n \leq 4$, and the balance between the Li−O bonds and hydrogen bonds becomes important in larger clusters. The first-shell hydration structure of the neutral Li atom is similar to that of Li^+ with the same $n \geq 4$. The *3-fold* structures which correspond to the *surface* structures of $Na(H_2O)_n$ are local minima even when n increases.

(2) The $Li(H_2O)_n$ is stabilized by 10.0−13.2 kcal/mol in energy and 8.1−12.0 kcal/mol in enthalpy (1 atm 298.15 K) by the stepwise hydration. The calculated successive enthalpies of $[Li(H_2O)_n]^+$ agree well with experiments. Though the interaction between Li and the first-shell ligands and that among the water molecules are important factors, the *intershell Li−water* interaction becomes more and more essential to form the stable neutral structure for $n \geq 5$. On the other hand, the electrostatic interactions between Li^+ and both the first- and the second-shell water molecules as well as the intershell hydrogen bonds are important in the hydrated Li^+ complexes.

(3) The calculated vertical IPs of the most stable *interior* $Li(H_2O)_n$ as a function of n is in good agreement with the recent experiment. They decrease monotonically until $n = 4$ and become almost constant, converging to the bulk limit of the VDE of $(H_2O)_n^-$ for $n \geq 4$.

(4) The electronic nature of the hydrated Li atom clusters changes from the one-center atomic state for $n \leq 3$ to the two-center ionic state for $n \geq 4$ with the gradual localization of the excess electron in the space on and between the outer second-shell waters. In the neutral clusters with more than four H_2O molecules, Li acts as a cation center and the excess electron becomes distributed not in the vicinity of Li but outside the first-shell cavity. The dangling hydrogens which do not take part in the hydrogen bonds but interact with the excess electron play a role as actuators of the *surface* state.

(5) The structures whose IPs are insensitive to the cluster size have the localized excess electron distribution in the surface region of the clusters. The surface ionization is considered to occur in these complexes.

Acknowledgment. The authors are grateful to Prof. Fuke and Dr. Takasu (Kobe University) for their valuable discussions. This work is financially supported by the Grant-in-Aid in Priority Area of "Chemistry of Small Particle Systems" (Nos. 07240224, 08230225, and 09216218) from the Ministry of Education, Science, Sports and Culture of Japan. All computations were carried out at the computer centers at Tokyo Metropolitan University and at the Institute for Molecular Science (IMS). We are grateful for the allotment of the computer time at IMS.

Supporting Information Available: Optimized structures for $Li(H_2O)_n$ ($n = 1-3$) (Figure S1), their selected geometrical parameters and total binding energies (Tables S1 and S2) calculated at various levels, and total gross population on Li s basis functions in $Li(H_2O)_n$ ($n = 1-8$) (Table S3) (5 pages, print/PDF). See any current masthead page for ordering information and Web access instructions.

JA972726+